Dynamic root growth in response to depth-varying soil moisture availability: a rhizobox study

Cynthia Maan[1], Marie-Claire ten Veldhuis[1], and Bas van de Wiel[1]

[1]Geoscience and Remote Sensing, Delft University of Technology, Stevinweg 1, 2628 CN Delft,The Netherlands

Correspondence: Cynthia Maan (dcmaan@gmail.com)

Abstract. Plant roots are highly adaptable, but their adaptability is not included in crop and land surface models. They rely on a simplified representation of root growth, independent of soil moisture availability. Data of subsurface processes and interactions, needed for model set-up and validation, are scarce. Here we investigated soil moisture driven root growth. To this end we installed subsurface drip lines and small soil moisture sensors (0.2 L measurement volume) inside rhizoboxes (length x width x height, 45 x 7.5 x 45cm). The development of the vertical soil moisture and root growth profiles are tracked with a high spatial and temporal resolution. The results confirm that root growth is predominantly driven by vertical soil moisture distribution, while influencing soil moisture at the same time. Besides support for the functional relationship between the soil moisture and the root density growth rate, the experiments also suggest that vertical root growth stops when the soil moisture at the root tip drops below a threshold value. We show that even a parsimonious one-dimensional water balance model, driven by the measured water input and output fluxes, can be convincingly improved by implementing root growth driven by soil moisture availability.

1 Introduction

Droughts are expected to become more severe and last longer, resulting in increasing (water) stress on plants. However, their dynamic growth provides the plants with a strong ability to adapt and develop resilience to droughts and climate change (Engels et al., 1994; Gao et al., 2014). Especially the flexibility of the root system can be crucial for the plants resilience to droughts and their natural adaptation strategies (King et al., 2003; Ristova and Barbez, 2018; Wasaya et al., 2018; Zhang et al., 2019; Wang et al., 2021). However, the flexibility of plant roots, and their ability to adapt to the environment, is badly included in crop and land surface models (Warren et al., 2015). At the same time, climate and ecosystem models poorly represent the fluxes of water and heat to the atmosphere (Giard and Bazile, 2000), are sensitive to the chosen vertical root distribution profiles (Feddes et al., 2001), and commonly underestimate the impact of the rooting depth on climate and climate change (He et al., 2004; van Dam et al., 2011; Warren et al., 2015).

In most crop and land surface models, the vertical root distribution is simply parameterized as an exponentially decaying function with soil depth (Feddes and Rijtema, 1972; Gerwitz and Page, 1974; Jackson et al., 1996; Kroes et al., 2009), while the maximum rooting depth is described by a linearly increasing function with time (Kroes et al., 2009), i.e. both independently of soil moisture. Some exceptional models treat root growth more dynamically by relating root growth to soil related parameters

as accumulated temperature or root zone soil moisture. Models that take the vertical profiles of soil moisture into account, however, are scarce. However, many studies indicate that in reality parameters as root length, penetration depth and depletion rate at depth are dominantly influenced by soil moisture (Barber et al., 1988; Coifman et al., 2005; Zhang et al., 2019), and that deviating functions and trends are commonly found in nature (Fan et al., 2017).

30   For maize and rape plants it was found that the plants respond rapidly to drying and re-wetting the topsoil by locally increasing root growth in soil layers with the most favourable conditions (Engels et al., 1994). The same study suggests that the plasticity in root growth contributes to the maintenance of an adequate nutritional status (Engels et al., 1994). For cotton, Klepper et al. (1973) were able to stimulate a maximum root length density deeper in the soil by altering irrigation schedules. For wheat plants, King et al. (2003) noted that greater density of fine roots at depth increases yields through access to additional

35 resources. Deeper roots lead to higher resilience to subsequent droughts, by increasing the root zone and water accessibility (King et al., 2003).

    Models for dynamical root growth have been proposed by Adiku et al. (1996) and Schymanski et al. (2008). Both models allow for enhanced root density growth in areas where soil water is more easily available. The model of Adiku et al. (1996) furthermore includes a proportional dependency of the root growth on the local root length density, while the bulk root growth

40 is linked to the bulk biomass growth (Adiku et al., 1996). The model was (only) qualitatively validated against root density measurements for two different scenarios: (1) for vertically homogeneous and non-limiting soil water conditions, in which case the model reproduced an exponential decline in root length density with increasing soil depth; and (2) for limiting soil water conditions with downward increasing water content, in which case the patterns of the simulated and observed root growth deviated from a simple exponential function, with more roots in the lower parts of the soil profile.

45   In the model of Schymanski et al. (2008), the bulk root density growth depends on the difference between the plants water demand and the actual water uptake: growth of the root bulk in case of water shortage and decay of the root bulk in case of water abundance. The distributions in the vertical are related to the soil moisture profiles. The model was validated against evapotranspiration data and soil moisture at 10 cm depth. Wang et al. (2018) implemented the model in the Noah land surface model and showed the importance of including flexible root growth for a correct representation of the water and energy fluxes.

50 A better understanding of the coupled action of plant roots and the subsurface environment could furthermore lead to the development of methods for system manipulation and boosting the plants climate resilience.

    To investigate the dominance of soil moisture driven root growth, we test a similar -but more parsimonious- root system model. The model is parameterized and validated based on data from an experimental set-up in a rhizobox including one soil-plant system. We use a similar root distribution function as Schymanski et al. (2008), but neglect the possible influence of

55 the plants water demand (or biomass growth rate) on the bulk root growth; note that the existing models are not unambiguous about the latter, since some models assume a positive effect of (moderate) water shortage on root growth, while others assume a negative effect of a (persistent) water shortage (through a reduced biomass growth rate). Probably parameters as plant type and the size of demand are decisive. In contrast to a 'demand-driven dependency', we here presume a 'supply-driven' bulk root growth, i.e. root growth (of both, the local and the bulk) is stimulated by soil moisture availability. To apply our exper-

60 imental set-up for model calibration and validation, we simulate a single soil-plant system. Hence, a direct comparison with

the experimental data is possible, and the model can be validated against both, measurements of the water balance components and root growth rates. Our model is characterized by simplicity; the water balance model requires the irrigation and (potential) evapotranspiration flux as system drivers, similar to Schymanski et al. (2008), and the following three calibration parameters: (1) the vertical root growth rate in saturated conditions, (2) the water extraction rate per root-centimeter in saturated conditions and (3) the root density growth rate in saturated conditions.

In the next chapter, we describe our experiments and model formulation. In Section 2.1, the experimental set-up is discussed. The results are used to define a diagnostic equation between root growth and soil moisture in section 2.2. Secondly, we combine the diagnostic equation with the Richard's equation and formulations for root water uptake (Section 2.3) and root density growth (Section 2.4) to link both system variables (i.e. root growth and soil moisture) to independent system drivers (Section and 2.4). In Chapter 3 conclusions are presented.

2 Experiments

2.1 Experimental Set-up

We study 50 days of evolution of a maize soil-root system inside a rhizobox (with a length x width x height of 45 x 7.5 x $45cm$, respectively), see Figure 1. Irrigation is supplied continuously at a low flow rate through porous drip lines (with an inside diameter of $4mm$) that were installed at five different levels (with $10cm$ intervals) at $1.5cm$ distance parallel to each window (see Figure 1). The flow rate is constant throughout the day, but adjusted in steps (in an attempt to follow the water demand of the plant, see the black and red dashed curves in Figure 2A). To control the verical soil moisture gradients and stimulate vertical root growth, the irrigation depth was increased over time to moisten the deeper soil layers one by one, see Figure 2D. Irrigation is applied at one depth at a time. The rhizobox was filled with a sifted black potting soil ('Pokon Universal Potting Soil', made up largely of peat moss) - sand mix (weight ratio 1:2.7). The soil moisture is measured continuously at four depths inside the rhizobox with ECH20 EC-5 Soil Moisture Sensors. Every few days the root growth is monitored by tracing the roots on a transparent sheet, through the transparent window. Subsequently, pictures were made of the transparant sheets and the *Fiji-ImageG* software was used to measure root lengths and (a proxi for) root densities (i.e. the total measured root length in each vertical centimeter, devided by the horizontal dimension of the rhizobox of $45cm$). At the bottom, a drainage reservoir was installed. The top soil was covered with plastic to prevent evaporation from the soil. The set-up was placed on a $1g$ precision scale (Mettler-Toledo MS32000Le/01) to track the overall water balance. It should be noted, however, that the total time series of the system mass, as plotted in Figure 2A, was subjected to multiple extrapolations from shorter time series (with time spans of hours to days), to deal with (daily) interruptions during the execution of the experiments. Furthermore, the increase in the plant's mass was neglected. The above-ground wet biomass was measured after the whole period to be 105 gram (determined by cutting the plant at ground level and measuring the corresponding weight change), which is small compared with the gross irrigation and evapotranspiration fluxes (typically about 100 gram daily), but significant compared with the net changes in the water balance. The weight measurements were mainly used to have an estimate for the evapotranspiration flux, which is compared with the simulations, and to determine the long-term water demand or abundance in order to adjust the

irrigation rate to what the plant needs. The experiment starts at $t = 0$ when a maize plant (which was sown around two weeks earlier in a small pot) with a maximum root length of $5cm$ and an above ground height of $10 - 15cm$ was placed inside the rhizobox.

2.2 Diagnostic model of root growth: root follows moisture

Time series and correlations

The soil moisture development is plotted together with profiles of the soil moisture and root density growth within succeeding periods in figure 2B-C. Root development is found to be most pronounced at depth intervals with highest soil moisture. These results suggest that soil moisture and root growth distributions are strongly connected.

Model formulation

We test the following diagnostic equation to model the root growth rate distributed as function of the (normalized) soil moisture:

$$\frac{\partial R}{\partial t}\frac{1}{r} = \frac{\theta_n}{\int_L^0 \theta_n dz}, \tag{1}$$

Where $R(z,t)$ (cm/cm^3) is the root density profile, θ_n is the normalized water content

$$\theta_n = \frac{\theta - \theta_w}{\theta_s - \theta_w}, \tag{2}$$

with θ_s the saturated water content and θ_w the wilting point, i.e. the minimum amount of water in the soil that is required for any water absorbance by the roots (Kirkham, 2005).

$r(t)$ in equation 1 is the depth integrated root growth:

$$r = \int_L^0 \frac{\partial R}{\partial t} dz, \tag{3}$$

with $L(t)$ (cm) the vertical rooting depth, which is assumed to increase linearly in time by a constant growth rate u_1:

$$\frac{\partial L}{\partial t} = u_1 \tag{4}$$

Hence, equation 1 links the local root growth tendency, normalized by the bulk growth tendency, to the local soil moisture, also normalized by the bulk soil moisture.

Model parameter evaluation and results

Modeled root growth profiles are compared with the experimental data for successive time periods, see Figure 3A-E. Note that the two dimensional root length density observed at the window (in cm/cm^2) is used as a direct proxy for the actual root length density $R(z,t)$ (cm/cm^3). For the results in Figure 3 and for the further experiments presented in this paper, the vertical root growth is taken as $u_1 = 5cm/day$ (based on observations). In Figure 4 the sensitivity to this parameter is investigated. For the wilting point we take $\theta_w = 0.075$ (Bleam, 2016; Rai et al., 2017). Patterns of root growth are represented fairly well (Figure 3), with the exception of the sharp local peak that occurs within the time slot $40 - 50$ days (at $z = -30$). This latter case is improved by adopting an extra condition for vertical root growth at the root tip: no vertical root growth occurs if the soil moisture at the root tip is smaller than $\theta = 0.075$ (see Figure 3).

2.3 Soil moisture and water uptake model

Model formulation

To calculate the evolution of the water content (θ) due to irrigation, soil water flow and plant water uptake, we apply Richards equation:

$$\frac{\partial \theta}{\partial t} = \frac{\partial q}{\partial z} - S + I \tag{5}$$

with S $(cm^3/cm^3/min)$ the soil water extraction by plant roots, I $(cm^3/cm^3/min)$ the irrigation, z (cm) the vertical coordinate, taken positively upward , and q (cm/min) the soil water flux density (positive upward) . q is given by Darcy's equation:

$$q = K(h)\frac{\partial(h+z)}{\partial z} \qquad , \tag{6}$$

with K (cm/min) the hydraulic conductivity and $h(cm)$ the soil water pressure head. Following (Clapp and Hornberger, 1978), h is taken as;

$$h = h_s \frac{\theta}{\theta_s}^{-b} \tag{7}$$

and K is taken as;

$$K = K_s \frac{\theta}{\theta_s}^{2b+3} \tag{8}$$

with h_s and k_s respectively the soil water pressure head (cm) and conductivity at saturation, θ_s the saturated water content and b an empirical exponent. The values of k_s, θ_s and b are taken from Clapp and Hornberger (1978), and correspond to loamy sand.

Following Adiku et al. (1996), the soil water extraction S is calculated by:

$$S = u_2 R \theta_n \tag{9}$$

Where u_2 is the water extraction rate per centimeter of roots in saturated conditions ($ml/cm/min$ or $cm^3/cm/min$), S the actual soil water extraction by plant roots per soil volume per minute ($ml/cm^3/min$), and $R(z,t)$ is the root length density, i.e. roots per soil volume (cm/cm^3).

Model parameter evaluation

The water extraction rate per centimeter of roots in saturated conditions u_2 is determined by comparing the soil moisture data with the soil moisture simulations driven by the root density data. The sensitivity to a range of tested variations are indicated in Figure 5. For figure 6 and the further experiments we take $u_2 = 1.2 \cdot 10^{-2} ml/cm/hr$, based on observation.

Results and discussion

Soil moisture and water uptake simulations were performed for the following settings for the root density profiles: (1) for the measured root profiles, (2) for the calculated root profiles, and (3) for exponential equivalents (most roots in the upper soil), all with identical (measured) overall root growth rates. Results are indicated in Figure 6. The first 10 days were omitted because of the lack of observable root growth; it takes a couple of days before the roots can be observed at the window.

The results indicate that the soil moisture profiles and water uptake profiles derived from the modeled root profiles correspond fairly well with the results obtained from the measured root profiles (comparison solid and dashed lines in Figure 6), whereas the results derived from the exponentially shaped profiles show larger deviations, especially for the periods 30-40 days and 40-50 days.

Furthermore, the simulations driven by the measured and modeled root profiles correspond better with the measured total uptake rates compared to the simulations driven with the exponentially shaped root profiles (see Table 1), except for the first period (10-20 days).

However, the differences between the modeled water components are relatively small, compared with the big differences in the root profiles. Even with the less realistic exponential root profiles, rather similar soil moisture profiles are found (Figure 6). In each panel, the local peaks in the soil moisture coincide with the depths of irrigation. Smaller local root densities at these depths correspond with higher and wider soil moisture peaks (compare the dashed and dotted profiles in Figure 6), which can simply be explained by the smaller local uptake rates. Note that wider peaks result in a larger area in which uptake by plant roots can occur. Hence, this positive effect on the water uptake rates implies a negative (regulating) feedback loop between these components of the water balance (i.e. higher soil moisture leads to more water uptake, which subsequently reduces soil moisture), which keeps the differences limited.

2.4 A prognostic model for coupled soil moisture and root growth

Model formulation

Soil moisture and root growth are interacting variables. To *prognostically* simulate the time evolution of both variables, we implement the following equation for root density growth in the model described in Section 2.3:

$$\frac{\partial R}{\partial t} = u_3 \theta_n. \tag{10}$$

Hence, the local root growth tendency is now normalized by the (static) root density growth in optimal conditions (saturation) u_3 ($cm/cm^3/min$), instead of by the (measurable) bulk root growth tendency in Equation 1. Equation 10 differs from the formulation proposed by Adiku et al. (1996), which includes a proportional dependency of the root growth on the local root length density. The simulations with the exponential equivalent are performed in a similar fashion: After each update of the root density profile, the exponential equivalent (with identical overall root length) is calculated and used for calculating the plant water uptake. The model is driven by irrigation data and the estimated overall evapotranspiration fluxes.

Model calibration

The root density growth in saturated soil u_3 is estimated by comparing the simulated root profiles with the data. The sensitivity to the tested variations are indicated in Figure 7. Based on the results in Figure 7, we take $u_3 = 0.2 cm/cm^3/day$ for the simulations in Figure 8.

Results and discussion

Also in a coupled fashion, driven by irrigation data and the estimated overall evapotranspiration fluxes, the modeled root profiles are clearly improvements to the exponential profiles (left column in Figure 8), except for the first 20 days during which the exponential profile seems to be a good approximation. Also the simulated soil moisture profiles (comparison of the data points with the dashed and dotted lines in the middle column of Figure 8) and the overall water extraction rates (Table 2) are slightly improved, although these differences might be smaller than expected from the relatively big differences in the root denisity distributions. Table 3 indicates that the exponential profiles resulted in larger overall (bulk) root lengths compared with the flexible profiles. Although the exponential shape is static and does not depend on the soil moisture profile, the bulk root growth rate depends linearly on the vertically integrated soil moisture field via equation 10: an off-shape profile initially results in higher vertically integrated soil moisture values, which triggers extra root growth. Hence, from a 'water balance perspective' an inefficient (unrealistic) profile shape gets compensated by extra root growth, which (in another way) points (again) to the relevance of including soil moisture dependent (bulk) root growth for realistic water balances. This is in contrast with the linear dependency of the overall root growth on the overall biomass growth (independently of soil moisture), which is often assumed in crop and land surface models.

3 Conclusions

Our results confirm that there is a strong, and dominant, influence of soil moisture on root density growth and vertical rooting depth. We show that root profiles can be predicted realistically from information on soil moisture profiles only. If soil moisture driven root growth is coupled to an infiltration model, both root and soil moisture profiles can be obtained based on water input and (potential) evapotranspiration fluxes, plus a few constants and simple principles, suggesting that the system could be rather insensitive to above ground processes and overall biomass growth. However, a detailed (crop specific) parameter study is needed to quantify the effect of model calibration, and for generalizing the results based on a single soil-plant system.

Our results also show that, in our modeled soil-plant system, the effect of unrealistic root profiles on the water balance components is partly compensated by e.g. spatial diffusion and soil pressure driven water flow redistribution. This means that missing information on the precise root distribution, does not automatically mean that large errors in the water budgets are made. However, in the latter case the correct water budget results from 'compensating' errors rather than from correct process mechanism.

This study treats root growth independent of above ground processes, while such a dependence is plausible. However, our results suggest that soil moisture status is a dominant factor influencing root growth. Underestimation of the impact of soil moisture on root growth rates, can result in underestimated plant resilience to drought and environmental changes. Regarding the resilience to drought stress, we suggest that continuous adequate root growth during periods of favorable soil moisture conditions, might be a strategy for plants to prevent water demand or water stress during dry periods.

The conceptual simplicity of our proposed model enables straightforward implementation in regional Land-Atmosphere models, to replace current exponential root profiles. The main benefits will be a more correct representation of soil-plant water fluxes, and a more realistic representation of root biomass, especially in situations where soil moisture availability is predominant in the deeper soil layers.

Code and data availability. The data for producing the graphs and results will be made available at https://doi.org/10.4121/19513957.

Author contributions. Cynthia Maan: conceptualization, experiments, code- and model design, writing - original draft, data curation. Marie-Claire and Bas van de Wiel: funding acquisition, supervision, writing - Review & Editing

Competing interests. one author is member of the editorial board of HESS. The peer-review process was guided by an independent editor, and the authors have also no other competing interests to declare.

225   *Acknowledgements.* This research was supported by the 4TU.Federation in the Netherlands via the 'High Tech for a Sustainable future' programme. We thank S. Schymanski and two anonymous reviewers for their constructive comments to improve the quality of the paper.

References

Adiku, S., Braddock, R., and Rose, C.: Modelling the effect of varying soil water on root growth dynamics of annual crops, Plant and soil, 185, 125–135, 1996.

Barber, S., Mackay, A., Kuchenbuch, R., and Barraclough, P.: Effects of soil temperature and water on maize root growth, Plant and Soil, 111, 267–269, 1988.

Bleam, W. F.: Soil and environmental chemistry, Academic Press, 2016.

Clapp, R. B. and Hornberger, G. M.: Empirical equations for some soil hydraulic properties, Water resources research, 14, 601–604, 1978.

Coifman, R. R., Lafon, S., Lee, A. B., Maggioni, M., Nadler, B., Warner, F., and Zucker, S. W.: Geometric diffusions as a tool for harmonic analysis and structure definition of data: Diffusion maps, Proceedings of the National Academy of Sciences of the United States of America, 102, 7426–7431, 2005.

Engels, C., Mollenkopf, M., and Marschner, H.: Effect of drying and rewetting the topsoil on root growth of maize and rape in different soil depths, Zeitschrift für Pflanzenernährung und Bodenkunde, 157, 139–144, 1994.

Fan, Y., Miguez-Macho, G., Jobbágy, E. G., Jackson, R. B., and Otero-Casal, C.: Hydrologic regulation of plant rooting depth, Proceedings of the National Academy of Sciences, 114, 10 572–10 577, 2017.

Feddes, R. A. and Rijtema, P. E.: Water withdrawal by plant roots, Journal of Hydrology, 17, 33–59, 1972.

Feddes, R. A., Hoff, H., Bruen, M., Dawson, T., De Rosnay, P., Dirmeyer, P., Jackson, R. B., Kabat, P., Kleidon, A., Lilly, A., et al.: Modeling root water uptake in hydrological and climate models, Bulletin of the American meteorological society, 82, 2797–2810, 2001.

Gao, H., Hrachowitz, M., Schymanski, S., Fenicia, F., Sriwongsitanon, N., and Savenije, H.: Climate controls how ecosystems size the root zone storage capacity at catchment scale, Geophysical Research Letters, 41, 7916–7923, 2014.

Gerwitz, A. and Page, E.: An empirical mathematical model to describe plant root systems, Journal of Applied Ecology, pp. 773–781, 1974.

Giard, D. and Bazile, E.: Implementation of a new assimilation scheme for soil and surface variables in a global NWP model, Monthly weather review, 128, 997–1015, 2000.

He, J., Wang, Z., and Fang, J.: Issues and prospects of belowground ecology with special reference to global climate change, Chinese Science Bulletin, 49, 1891–1899, 2004.

Jackson, R., Canadell, J., Ehleringer, J. R., Mooney, H., Sala, O., and Schulze, E. D.: A global analysis of root distributions for terrestrial biomes, Oecologia, 108, 389–411, 1996.

King, J., Gay, A., Sylvester-Bradley, R., Bingham, I., Foulkes, J., Gregory, P., and Robinson, D.: Modelling cereal root systems for water and nitrogen capture: towards an economic optimum, Annals of botany, 91, 383–390, 2003.

Kirkham, M.: Field capacity, wilting point, available water, and the non-limiting water range, Principles of soil and plant water relations, 8, 101–115, 2005.

Klepper, B., Taylor, H., Huck, M., and Fiscus, E.: Water Relations and Growth of Cotton in Drying Soil 1, Agronomy Journal, 65, 307–310, 1973.

Kroes, J., Van Dam, J., Groenendijk, P., Hendriks, R., and Jacobs, C.: SWAP version 3.2. Theory description and user manual, Tech. rep., Alterra, 2009.

Rai, R. K., Singh, V. P., and Upadhyay, A.: Planning and evaluation of irrigation projects: methods and implementation, Academic press, 2017.

Ristova, D. and Barbez, E.: Root Development: Methods and Protocols, Springer, 2018.

Schymanski, S. J., Sivapalan, M., Roderick, M. L., Beringer, J., and Hutley, L. B.: An optimality-based model of the coupled soil moisture
265   and root dynamics, Hydrology and earth system sciences, 12, 913–932, 2008.

van Dam, J., Metselaar, K., Wipfler, E., Feddes, R., van Meijgaard, E., and van den Hurk, B.: Soil moisture and root water uptake in climate
models. Research Programme Climate Changes Spatial Planning, Tech. rep., WUR+ Royal Netherlands Meteorological Institute, 2011.

Wang, P., Niu, G.-Y., Fang, Y.-H., Wu, R.-J., Yu, J.-J., Yuan, G.-F., Pozdniakov, S. P., and Scott, R. L.: Implementing dynamic root optimiza-
tion in Noah-MP for simulating phreatophytic root water uptake, Water Resources Research, 54, 1560–1575, 2018.

270   Wang, Y., Zeng, Y., Yu, L., Yang, P., Van der Tol, C., Yu, Q., Lü, X., Cai, H., and Su, Z.: Integrated modeling of canopy photosynthesis,
fluorescence, and the transfer of energy, mass, and momentum in the soil–plant–atmosphere continuum (STEMMUS–SCOPE v1. 0.0),
Geoscientific Model Development, 14, 1379–1407, 2021.

Warren, J. M., Hanson, P. J., Iversen, C. M., Kumar, J., Walker, A. P., and Wullschleger, S. D.: Root structural and functional dynamics in
terrestrial biosphere models–evaluation and recommendations, New Phytologist, 205, 59–78, 2015.

275   Wasaya, A., Zhang, X., Fang, Q., and Yan, Z.: Root phenotyping for drought tolerance: a review, Agronomy, 8, 241, 2018.

Zhang, J., Wang, J., Chen, J., Song, H., Li, S., Zhao, Y., Tao, J., and Liu, J.: Soil Moisture Determines Horizontal and Vertical Root Extension
in the Perennial Grass Lolium perenne L. Growing in Karst Soil, Frontiers in plant science, 10, 629, 2019.
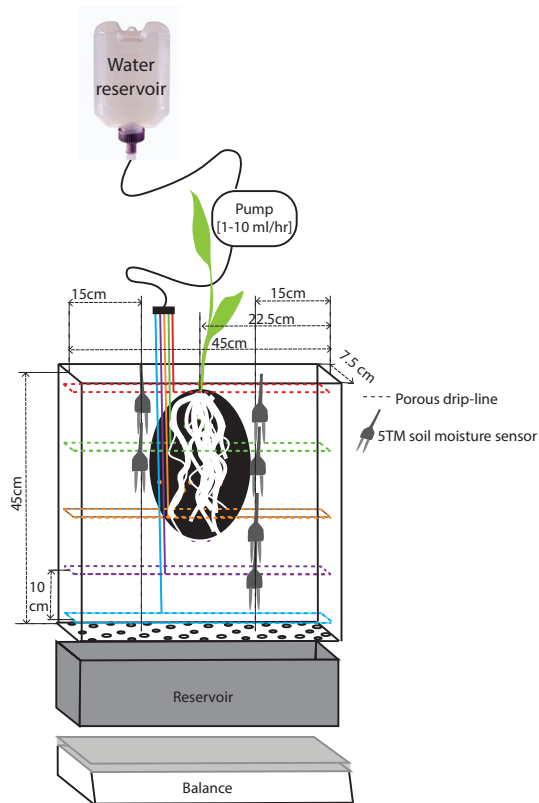
Figure 1. Schematic representation of the experimental setup inside a rhizobox. The collored dashed lines represent the drip lines at the different levels.

Table 1. Ratios of the calculated bulk water uptake rates (i.e. vertically integrated) to the measured bulk water uptake rates (derived from the mass balance). Calculations of the bulk water uptake are based on measured, modeled or exponential root profiles.

period	measured	modeled	exponent
10-20 days	0.77	0.81	0.75
20-30 days	1.01	0.96	0.83
30-40 days	1.1	1.1	0.89
40-50 days	0.95	0.95	1.2
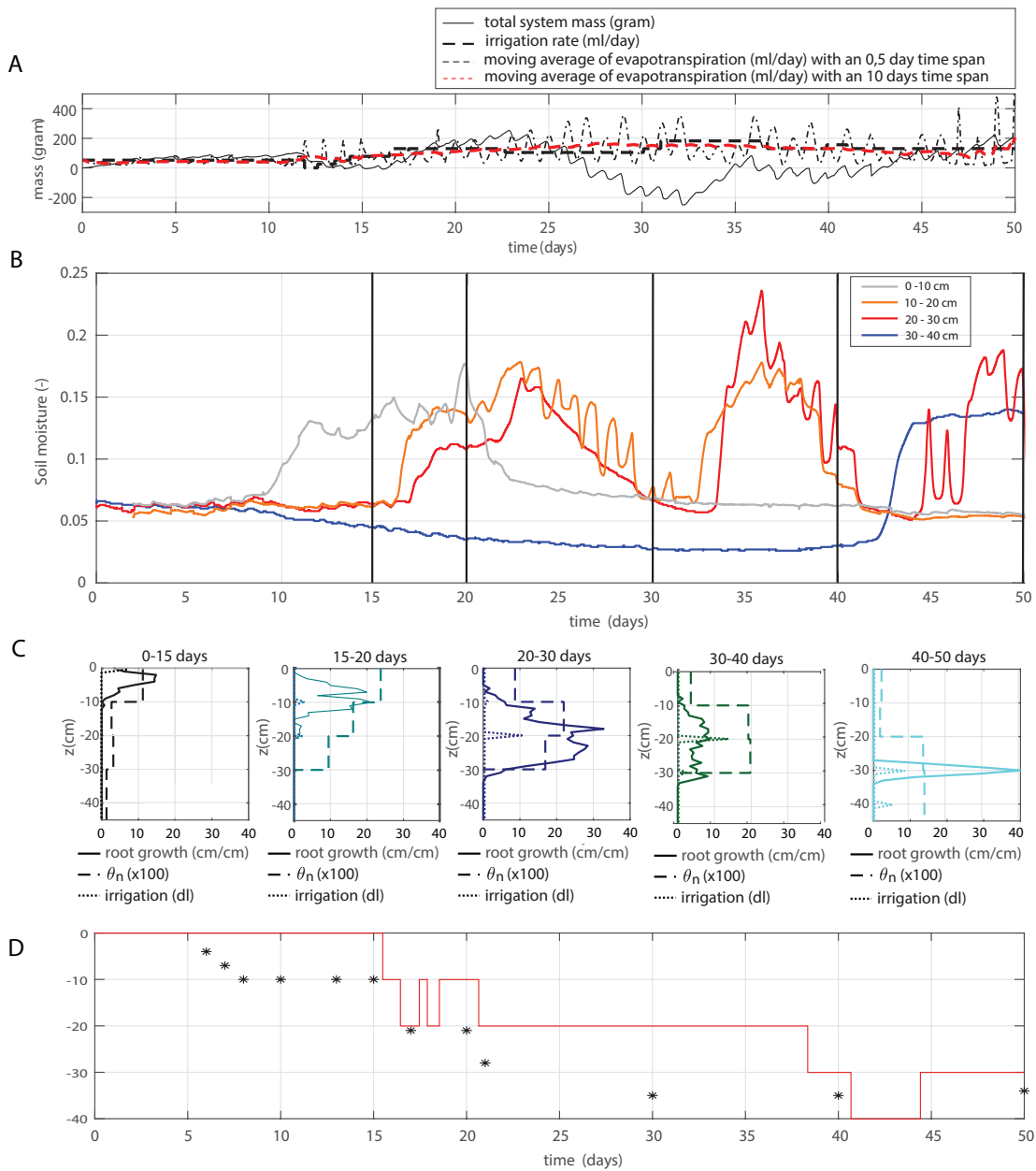
Figure 2. A: time series of the overall system mass, irrigation rate and evapotranspiration. B: time-series of the soil moisture within four different depth intervals. C: total root length that appears in the considered time frame (solid lines), time-averaged soil moisture profiles (dashed lines) and total applied irrigation volume (dotted lines). Root development is most pronounced in the intervals with largest soil moisture. D: applied irrigation depth (red line) and observed maximum rooting depth (markers).

Table 2. Ratios of the calculated bulk water uptake rates (i.e. vertically integrated) to the measured bulk water uptake rates (derived from the mass balance). Calculations of the bulk water uptake are based on simulations with the coupled model with flexible root profiles or exponential root profiles.

period	modeled	exponent
10-20 days	0.85	0.82
20-30 days	0.82	0.60
30-40 days	1.14	1.07
40-50 days	1.14	1.32

Table 3. Percentage increase in the total modeled root length in case of exponential profiles instead of dynamic root profiles.

period	difference
10-20 days	+2%
20-30 days	+20%
30-40 days	+51%
40-50 days	+54%
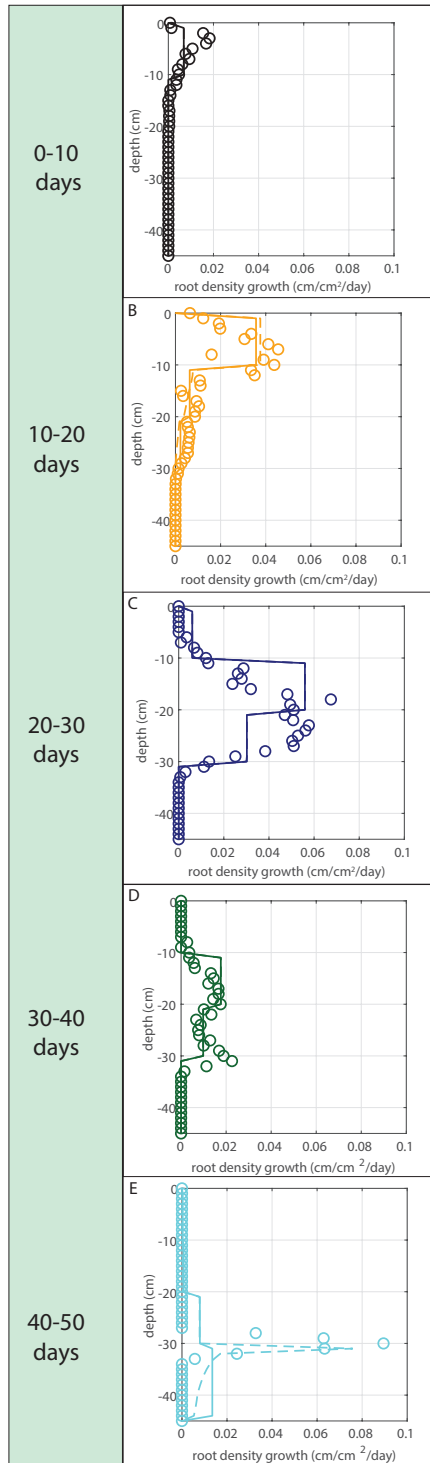
Figure 3. Vertical profiles of averaged root growth rates within succeeding periods as observed (circles) and as diagnostically calculated by equation 1 ('roots follow moisture principle', solid lines), using the measured bulk root growth and soil moisture profiles. Dashed lines are simulations with a threshold for root growth: $\theta > 0.075$. **15**
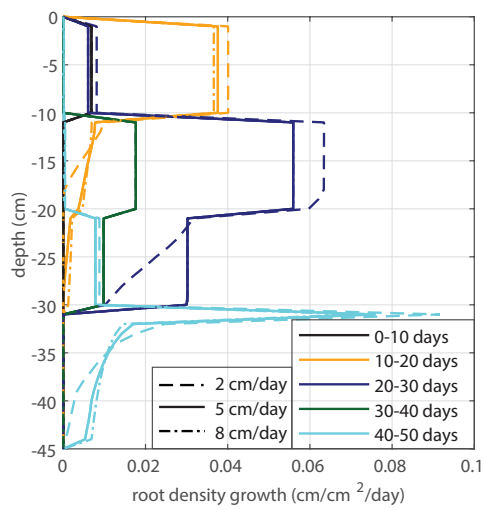
Figure 4. Sensitivity of root growth profiles to different values of the vertical root growth rate u_1. The different colors refer to the consecutive time periods of figure 3, i.e. the graphs represent 10-day averages of the daily root denisity growth rates.
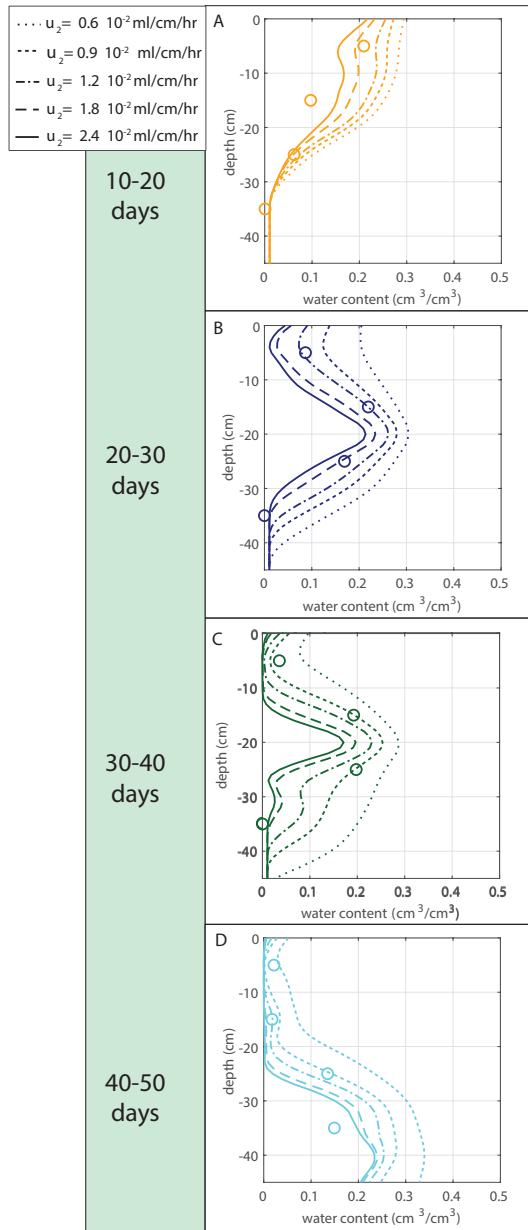
Figure 5. Sensitivity analysis for the water extraction rate in saturated conditions u_2

○   observed root profiles (left column) and soil moisture measurements (middle column)
—   simulations driven by measured root profiles.
—   simulations driven by the modeled root profiles (of Fig. 3).
– – & ·····   simulations driven by (two different) exponential profiles.
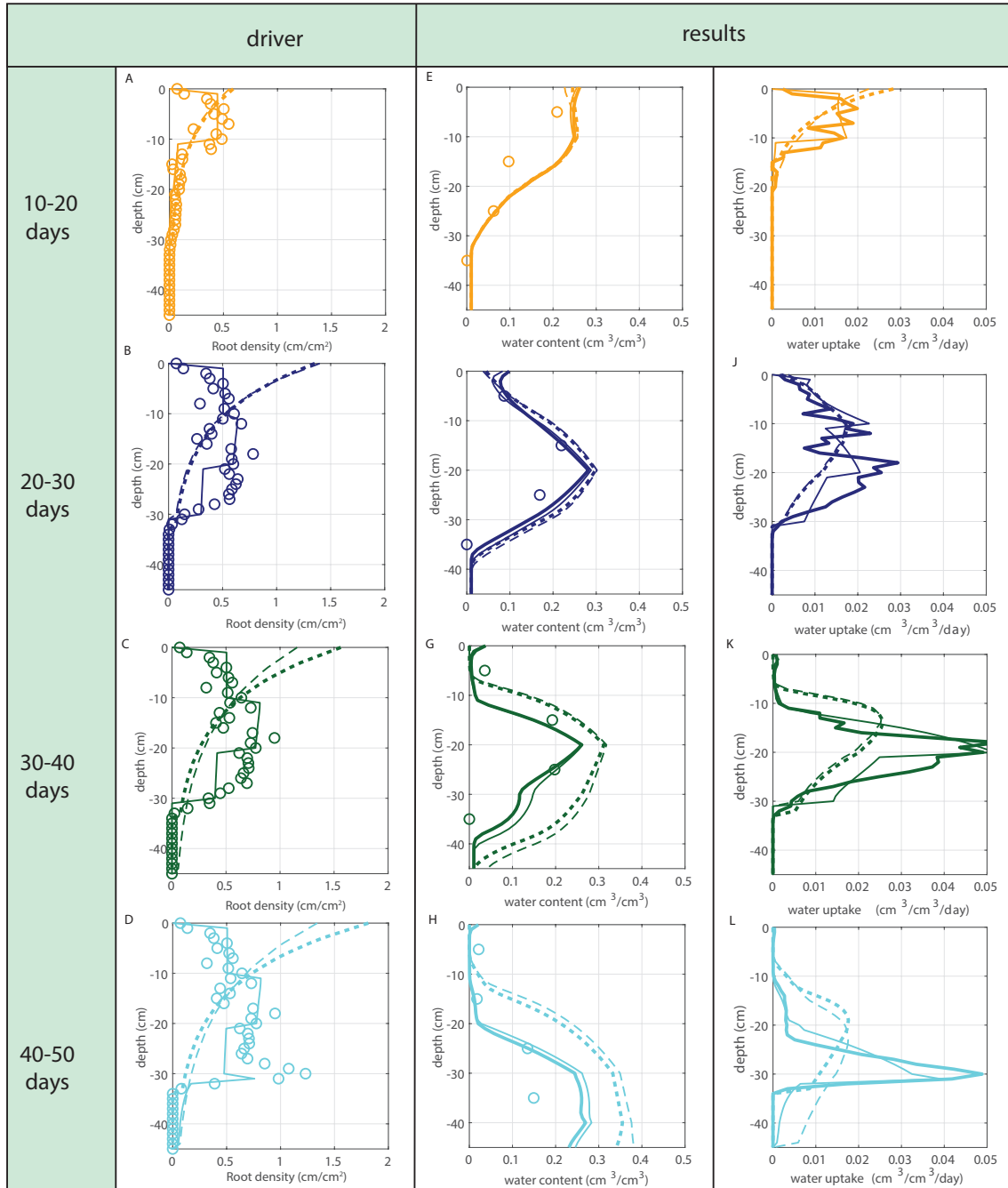
Figure 6. Offline simulations of time averaged soil moisture (middle column) and water uptake (right column) for the measured root profiles at the start of each period, for the calculated root profiles, and for exponential equivalents.
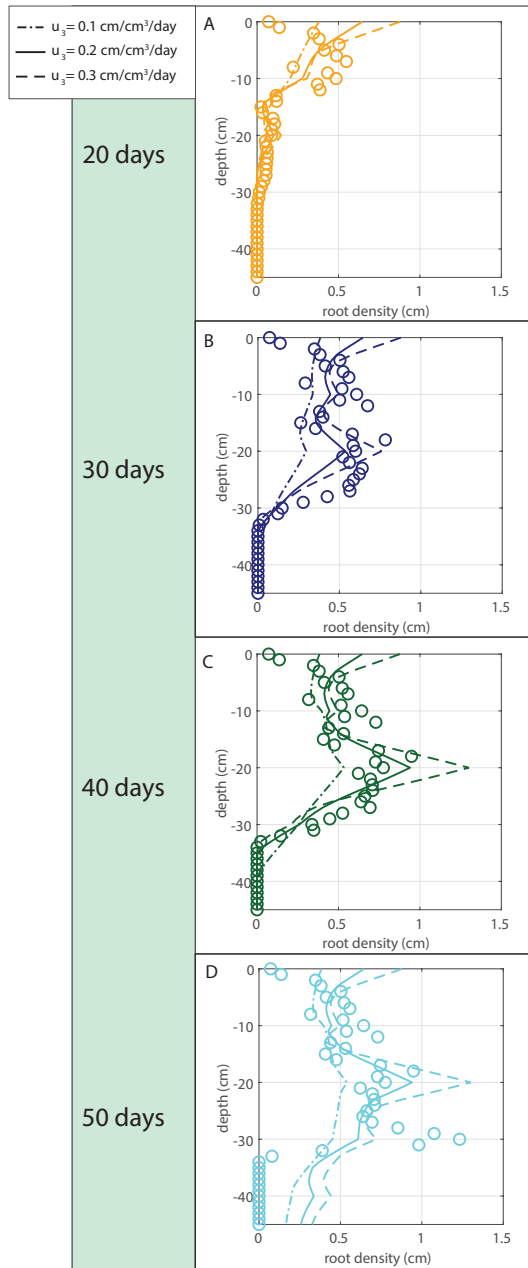
Figure 7. Sensitivity analysis for the root density growth rate in optimal (saturated) conditions u_3.
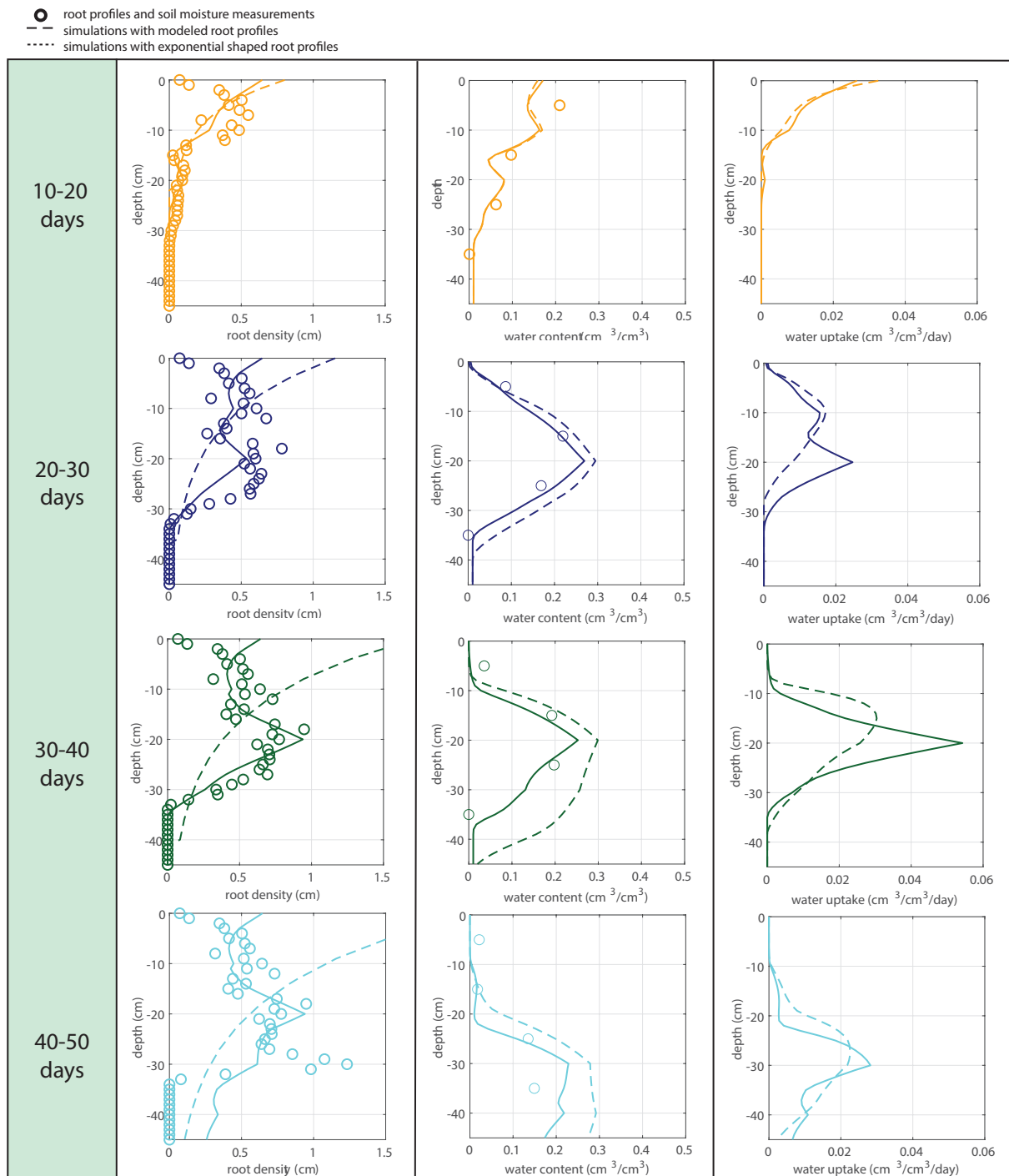
Figure 8. Fully coupled model with irrigation and evaporation as input parameters. Left: Observed (circles), simulated (dashed lines), and exponential (dotted lines) root profiles (at the start of each period). Middle: corresponding soil moisture profiles. Right: simulated uptake profiles for simulated and exponentially shaped root profiles.